Available online at www.sciencedirect.com

ScienceDirect

IFAC PapersOnLine 56-2 (2023) 126–131

Subdomain Fault Isolation for Linear Parameter Varying Systems through Coupled Marginalized Particle and Kitanidis Filters

Neha Aswal * **Eshwar Kuncham** * **Subhamoy Sen** *
Laurent Mevel **

* *i4S Laboratory, Indian Institute of Technology, Mandi, HP 175005 India (e-mail: d19035@students.iitmandi.ac.in, d19047@students.iitmandi.ac.in, subhamoy@iitmandi.ac.in).*
** *Univ. Gustave Eiffel, Inria, Cosys-SII, I4S, Campus de Beaulieu, Rennes 35042, France (e-mail: laurent.mevel@inria.fr)*

Abstract: Typically, for linear parameter varying systems, which can potentially get influenced by spatio-temporal external parameters, possible changes in their eigenstructure are not easy to be attributed conclusively to system faults or spatio-temporal parametric variations. Such spatio-temporal variations can although be estimated alongside, yet at the cost of making the estimable system dimension disproportionately large. Such augmented system dimension can thereby jeopardize tracking of the system evolution, either due to computational constraints or due to insufficient measurement channels (ill-posedness). This paper proposes a localized estimation approach wherein only a subdomain of the entire system is considered which reduces the dimension of the estimated model within manageable limits. To focus on the subdomain properties without knowledge of the rest of the model parameterization, a robust algorithm is developed through output injection using a simpler and sub-optimal version of Kitanidis filtering approach to induce robustness in the system parameter estimation against the boundary measurements. Finally, the subdomain model is estimated employing a marginalized filtering approach wherein a particle filter is employed for estimating both the eigenstructure and the controlling parameter while an ensemble Kalman filter estimates the states. The approach is demonstrated with the help of a mechanical system under spatial variation in temperature for which subdomain isolation necessitates the interface to be measured. In the context of the numerical application, the induced fault is due to damage, and the mechanical model is controlled and parameterized by the internal temperature, whose variations can be significant due to substantial external thermal variations inducing significant variations in the dynamic properties.

Keywords: Bayesian filtering, fault detection and isolation, vibration and modal analysis, linear parameter varying systems, dynamic substructuring, temperature variation.

1. INTRODUCTION

Success and efficiency for typical Bayesian filtering approaches for linear parameter varying (LPV) system estimation depend majorly on the system dimension (i.e., state/parameter dimension) and the available measurements. To ensure a smooth, accurate, and convergent estimation, the state dimension has to be judiciously chosen with respect to the possible output dimension. A very high dimensional state can, in fact, induce severe ill-posedness in the estimation leading to divergent and, at times, completely unreliable estimation. This aspect of Bayesian filtering appears when too many parameters are to be estimated using relatively less measurement/output information.

Linear systems for which the parameters are varying both in time and space is one such case wherein such scenarios can be experienced. With more severity in the spatial variation, the dimension of the parameters has to be enlarged in order to capture the parameter variation minutely. Eventually, this can make the problem extremely ill-posed provided the output dimension is not enhanced accordingly. Enhancing output resolution can also increase the problem dimension and make it slow, intractable, or divergent, and decrease promptness, posing challenges, especially for cases where promptness is the major objective to achieve.

Bayesian filtering-based Structural Health Monitoring (SHM), where the objective is the prompt assessment of the integrity (health) of a mechanical structure under thermal variation, is an excellent example case where such challenges can be encountered. From 2000 until

⋆ This study is partially funded by Aeronautics Research and Development Board, New Delhi, India, through grant file no. ARDB/01/1052042/M/I.

10.1016/j.ifacol.2023.10.1557

now, vibration-based damage diagnosis methods have been tested and evaluated for SHM of civil engineering structures. Cost and time-intensive visual inspections need to be replaced but with sufficient efficiency and automation through real-time Bayesian filtering-based SHM approaches to guarantee the safety and robustness of the considered infrastructure. Research has been conducted to apply such methods in continuous monitoring projects (refer to Carden and Fanning (2004)).

Moreover, *in-situ* systems suffer from the severe change in environmental conditions, conditions that are unmeasured, unknown, and non-stationary, while their impact on the structural performance is significant (Sohn, 2007; Deraemaeker et al., 2008). More robust SHM methods need to be developed to handle this impact on the structural integrity to avoid or reduce false alarm scenarios. Temperature, to which civil infrastructures are mostly exposed, is one such aspect that is considered to affect the structural performance, sometimes more than typical damages from the perspective of both magnitude and frequency (Liu and DeWolf, 2007). Handling the unknown temperature field information within a fault detection algorithm is, however, an unresolved primary concern in developing efficient and robust fault isolation and estimation approaches.

Many attempts at developing robust methods have been considered, most often relying on the comparison and regression of identified eigenstructure with respect to temperature (Sohn, 2007) and thereby increasing the demand for prior model simulation. Nevertheless, estimation still depends on the parameterization resolution and thereby may end up being compute-intensive to achieve sufficient accuracy and sometime ill-posed leading to infeasible estimation because of excessive parameterization- a perfect demonstration case for the LPV estimation problem discussed previously.

The current paper, therefore, presents a novel subdomain estimation approach for the LPV system wherein the system is locally identified (and thereby reduces parameter dimension) using Bayesian filtering tools. For this, instead of considering the whole system model in the fault detection procedure, a spatially local estimation approach is employed for only a subdomain of the whole model. Accordingly, the subdomain has to be isolated from the rest of the system taking into account the respective boundary conditions. Eventually, the boundary/interface needs to be measured and supplied to render the subsystem estimation independent of the rest of the system. Yet, not always the interface can be made available to be measured. Moreover, this inherently demands extensive output coverage, which may further escalate the cost.

This proposal, therefore, exploits the output injection approach described in Zhang and Zhang (2018) to make the overall approach robust to the lack of interface measurements. Since the interface does not need to be measured anymore, and the local monitoring is independent of the rest of the structure, the problem dimension gets reduced circumventing the need for extensive instrumentation.

Finally, both the external controlling parameter (here the temperature in each subdomain), the system eigenstructure (here the finite element model), and its restriction to the considered subdomain, are estimated jointly with the states through a particle filter. A special kind of particle filter was designed to handle problems where the system evolution was partly linear and partly non-linear. In such a so-called marginalized particle filter (MPF) or Interacting Particle Kalman Filter (IPKF) (refer to Schon et al. (2005); Karlsson et al. (2005); Zghal et al. (2014)), the linear part is estimated recursively by a Kalman filter (or its linear variants), whereas the non-linear part is tracked by a particle filter, reducing the overall burden of the online estimation. In this bank of Kalman filters, each Kalman filter is associated with a given particle, whose purpose is to estimate and track both the eigenstructure and parameter evolution.

The current paper is divided as follows. Section 2 describes the underlying model, Section 3 introduces the physical modeling, and Section 4, the identification algorithm. Finally, Section 5 presents a numerical simulation of a simple beam-mechanical system for illustration.

2. SUBDOMAIN STATE-SPACE FORMULATION

A subdomain Ω^s can always be isolated from the overall system domain Ω complementing with proper inputs in its boundaries, Koh et al. (1991). Accordingly, the discrete-time state-space model for an LPV subdomain at k^{th} time step is given by,

$$\begin{aligned} \mathbf{x}^s_{k+1} &= \mathbf{A}^s_k\mathbf{x}^s_k + \mathbf{B}^s_k\mathbf{u}^s_k + \mathbf{v}^s_k \\ \mathbf{y}^s_k &= \mathbf{H}^s_k\mathbf{x}^s_k + \mathbf{D}^s_k\mathbf{u}^s_k + \mathbf{w}^s_k \end{aligned} \tag{1}$$

where, $\mathbf{A}$, $\mathbf{B}$, $\mathbf{H}$, and $\mathbf{D}$ are the state transition, input, output, and direct transmission matrix, respectively. All these system matrices are assumed to be time-varying due to their dependence on certain parameters, Θ, varying spatially as well as temporally which, for brevity, has been omitted from Equation (1). The input and output vectors are given by $\mathbf{u}_{r\times 1}$ and $\mathbf{y}_{p\times 1}$, respectively, where r and p are the numbers of input and measurement channels for Ω^s. $\mathbf{v} \in \mathbb{R}^n$ and $\mathbf{w} \in \mathbb{R}^p$ are the process and measurement uncertainty terms, defined as stationary independent white Gaussian noises (SWGN) accounting for model inaccuracies and measurement noises, with their respective covariance $\mathbf{Q}^s$ and $\mathbf{R}^s$. The superscript s attributes the corresponding entities' association to the subdomain Ω^s.

The internal (i) and boundary (b) variables of the subdomain can further be segregated and the process equation can be represented as,

$$\begin{bmatrix}\mathbf{x}_i\\ \mathbf{x}_b\end{bmatrix}^s_{k+1} = \begin{bmatrix}\mathbf{A}_{ii} & \mathbf{A}_{ib}\\ \mathbf{A}_{bi} & \mathbf{A}_{bb}\end{bmatrix}^s_k \begin{bmatrix}\mathbf{x}_i\\ \mathbf{x}_b\end{bmatrix}^s_k + \begin{bmatrix}\mathbf{B}_{ii} & \mathbf{B}_{ib}\\ \mathbf{B}_{bi} & \mathbf{B}_{bb}\end{bmatrix}^s_k \begin{bmatrix}\mathbf{u}_i\\ \mathbf{u}_b\end{bmatrix}^s_k + \begin{bmatrix}\mathbf{v}_i\\ \mathbf{v}_b\end{bmatrix}^s_k \tag{2}$$

Upon segregating the entities corresponding to the internal variables (${\mathbf{x}_i}^s_k$ and ${\mathbf{u}_i}^s_k$) of Ω^s from the boundary variables (${\mathbf{x}_b}^s_k$ and ${\mathbf{u}_b}^s_k$), the equation can be recast for only internal variables of the subdomain with boundary effects as external input, ${\mathbf{q}_b}^s_k(= [{\mathbf{x}_b}^s_k; {\mathbf{u}_b}^s_k])$ and ${\mathbf{E}_{ib}}^s_k(= [\mathbf{A}_{ib}\ \mathbf{B}_{ib}]^s_k)$ being the corresponding input matrix,

$${\mathbf{x}_i}^s_{k+1} = {\mathbf{A}_{ii}}^s_k{\mathbf{x}_i}^s_k + {\mathbf{B}_{ii}}^s_k{\mathbf{u}_i}^s_k + {\mathbf{E}_{ib}}^s_k{\mathbf{q}_b}^s_k + {\mathbf{v}_i}^s_k \tag{3}$$

Accordingly, the measurement equation for Ω^s can be written as,

$${\mathbf{y}_i}^s_k = {\mathbf{H}_{ii}}^s_k{\mathbf{x}_i}^s_k + {\mathbf{D}_{ii}}^s_k{\mathbf{u}_i}^s_k + {\mathbf{L}_{ib}}^s_k{\mathbf{q}_b}^s_k + {\mathbf{w}_i}^s_k \tag{4}$$

with $\mathbf{L}_{ib}$ is the direct transmission term corresponding to the boundary input ${\mathbf{q}_b}^s_k$.

3. PHYSICAL PARAMETER MODELLING

Taking basis on the state-space formulation described above, and applying it specifically to a mechanical system, the eigenstructure of the system can be parameterized with the component system matrices, i.e., mass ($\mathbf{M}$), stiffness ($\mathbf{K}$), and damping ($\mathbf{C}$) matrices. While mass for typical structures mostly remains constant, damage can surely induce changes in stiffness and subsequently in damping (assuming it to be stiffness dependent). For a typical structure, stiffness depends on its material (elasticity, E, density, ρ, etc.) and geometric (length, l, area, a, etc.) properties. Spatial variation in temperature can incur changes in the material (and/or geometric) properties like elasticity and subsequently to the localized stiffness. Further, induced damage can alter the stiffness through elasticity deterioration. In order to address these variations in stiffness, localized stiffness (say stiffness E_m for m^{th} discretized element) can be parameterized by a health index (θ_m^E) and the internal temperature (θ_m^T) simultaneously as,

$$E_m = E(\theta_m^E, \theta_m^T) \tag{5}$$

Being a health index for the m^{th} element, θ_m^E assumes values within a range of $[0 \;\; 1]$ denoting two extreme health states: fully damaged and undamaged. The argument θ_m^T denotes the dependency of the element elasticity on the local temperature T. It has to be mentioned that the changes in dynamics due to temperature is reversible and benign and as such do not harm the structural integrity, unlike the other alterations due to material deterioration. Yet, such temperature-induced changes in dynamics can potentially cause a false alarm. There have been several numerical and physical experiments to investigate a material's behavior under thermal variation leading to several correlations between elasticity and temperature. This experiment adopts one such study by Kankanamge and Mahendran (2011), and the mentioned relation has been defined for a particular θ^E as,

$$E_m(\theta_m^E, \theta_m^T) = (-0.000835T + 1.0167)E_{m_{20}}(\theta_m^E) \tag{6}$$

where $E_{m_{20}}$ is the modulus of the member elasticity at $20°C$ and $T = 20°C + \Delta T$.

Assuming linear thermal expansion in the adopted structure, wherein the length dimension is comparatively larger than the other two (areal), the functional dependency of the element length, l_m, to T, is given by

$$l_m = l_{m_o}(1 + \alpha \Delta T) \tag{7}$$

with, l_m and l_{m_o} referencing the temperature at T_o ($= 20°C$) and $(T + \Delta T)$ respectively and α is the thermal expansion coefficient.

Finally, the governing differential equation (gde) of the system dynamics and its dependency on temperature T, can be demonstrated as,

$$\mathbf{M}\ddot{x}(t) + \mathbf{C}(t,T)\dot{x}(t) + \mathbf{K}(t,T)x(t) = \mathbf{f}(t) \tag{8}$$

where, $\mathbf{f}$ is the external force and $\{x, \dot{x}, \ddot{x}\}$ are displacement, velocity, and acceleration responses, respectively, corresponding to all degrees of freedom (dofs) of the system.

For the present study, a subdomain of the above system is, however, isolated and discretized in time, and the corresponding state-space model is prepared following Equations (3) and (4) wherein, $\mathbf{x}_i^s = \begin{bmatrix} x_i^s \\ \dot{x}_i^s \end{bmatrix}$, $\mathbf{A}_{ii}^s = \begin{bmatrix} \mathbf{0} & \mathbf{I} \\ -\mathbf{M}_{ii}^{s\,-1}\mathbf{K}_{ii}^s & -\mathbf{M}_{ii}^{s\,-1}\mathbf{C}_{ii}^s \end{bmatrix}$, $\mathbf{B}_{ii}^s = \begin{bmatrix} \mathbf{0} \\ \mathbf{M}_{ii}^{s\,-1} \end{bmatrix}$, $\mathbf{E}_{ib}^s = \begin{bmatrix} \mathbf{0} \\ -(\mathbf{M}_{ii}^{s\,-1}\mathbf{M}_{ib}^s + \mathbf{K}_{ii}^{s\,-1}\mathbf{K}_{ib}^s) \end{bmatrix}$, $\mathbf{u}_i^s = \mathbf{f}_i^s$, $\mathbf{q}_b^s = \ddot{x}_b^s$, $\mathbf{H}_{ii}^s = \begin{bmatrix} -\mathbf{M}_{ii}^{s\,-1}\mathbf{K}_{ii}^s & -\mathbf{M}_{ii}^{s\,-1}\mathbf{C}_{ii}^s \end{bmatrix}$, $\mathbf{D}_{ii}^s = \mathbf{M}_{ii}^{s\,-1}$, and, $\mathbf{L}_{ib}^s = -\mathbf{M}_{ii}^{s\,-1}\mathbf{M}_{ib}^s$, where index t and T are omitted for simplicity and to focus on the subdomain description.

It should, hereby, be mentioned that the measurement $\mathbf{y}_i^s$ is the total acceleration (relative and quasi-static) of the internal dofs of the subdomain. For details of this derivation, refer to Koh et al. (1991). This is to be noted that, the evaluation of one such subdomain at a time surely minimizes the overall problem dimension as well as the required measurement density, Koh et al. (1991).

4. METHODOLOGY

From Equations (3) and (4), it is evident that the estimation of states and measurement in the subdomain is dependent on its boundary conditions. To make the subdomain parameter estimation standalone, the boundary conditions should be known/computed or this requirement eliminated. Zhang and Zhang (2018) implemented a suboptimal variant of Kitanidis filter (Kitanidis (1987)) to cancel the influence of unknown non-stationary input excitation which is further validated for mechanical structures in Sen et al. (2021). This article takes the basis of this output injection approach in order to cancel the influence of the unknown boundary conditions resulting from the subdomain partitioning of the whole system. The current study, however, had to deal with additional direct transmission terms owing to boundary forces which have been addressed by projecting the real measurement orthogonal to the direct transmission.

Eventually, the induced robustness to boundary forces allows the subdomain to be treated as any other system for which the states and parameters are estimated employing marginalized/interacting filtering technique (refer to Schon et al. (2005); Karlsson et al. (2005) or Sen et al. (2021) for applications in mechanical engineering). The present study employs a variant of this marginalized particle filter family, wherein the location-based Θ are estimated by the particle filter (PF) while the states are estimated employing the ensemble Kalman filter (EnKF) nested within the PF. The following subsections explain the robustness induction procedure in detail.

4.1 Rejection of boundary conditions

In order to remove the dependency of the measurement equation, (cf. Equation (4)) on the boundary measurements, $\mathbf{q}_{b_k}^s$, the real measurement is projected orthogonal to $\mathbf{q}_{b_k}^s$, using a transformation matrix $\mathbf{T}_k^s$ that ensures $\mathbf{T}_k^s\mathbf{L}_k^s = 0$. The reduced measurement equation is obtained as follows,

$$\mathbf{z}_k^s = \widetilde{\mathbf{H}}_k^s\mathbf{x}_k^s + \widetilde{\mathbf{D}}_k^s\mathbf{u}_k^s + \widetilde{\mathbf{w}}_k^s \tag{9}$$

where, $\mathbf{z}_k^s = \mathbf{T}_k^s\mathbf{y}_k^s$, $\widetilde{\mathbf{H}}_k^s = \mathbf{T}_k^s\mathbf{H}_k^s$, $\widetilde{\mathbf{D}}_k^s = \mathbf{T}_k^s\mathbf{D}_k^s$, and $\widetilde{\mathbf{w}}_k^s = \mathbf{T}_k^s\mathbf{w}_k^s$. Subscripts, i, and b are dropped hereon for better readability.

Further, for any bounded non-zero matrix $\mathbf{G}^s_{k+1}$, Equation (3) is redefined taking basis on Equation (9) as,

$$\begin{aligned}\mathbf{x}^s_{k+1} =&\mathbf{A}^s_k\mathbf{x}^s_k + \mathbf{B}^s_k\mathbf{u}^s_k + \mathbf{E}^s_k\mathbf{q}^s_k + \mathbf{v}^s_k \\ &+ \mathbf{G}^s_{k+1}(\mathbf{z}^s_{k+1} - \widetilde{\mathbf{H}}^s_{k+1}\mathbf{x}^s_{k+1} - \widetilde{\mathbf{D}}^s_{k+1}\mathbf{u}^s_{k+1} - \widetilde{\mathbf{w}}^s_{k+1}) \\ =&\widetilde{\mathbf{A}}^s_k\mathbf{x}^s_k + \widetilde{\mathbf{B}}^s_k\mathbf{u}^s_k - \mathbf{G}^s_{k+1}\widetilde{\mathbf{D}}^s_{k+1}\mathbf{u}^s_{k+1} + \mathbf{G}^s_{k+1}\mathbf{z}^s_{k+1} + \widetilde{\mathbf{v}}^s_k\end{aligned} \tag{10}$$

wherein, $\widetilde{\mathbf{A}}^s_k = \mathcal{L}_k\mathbf{A}^s_k, \widetilde{\mathbf{B}}^s_k = \mathcal{L}_k\mathbf{B}^s_k, \widetilde{\mathbf{E}}^s_k = \mathcal{L}_k\mathbf{E}^s_k$, and $\widetilde{\mathbf{v}}^s_k = \mathcal{L}_k\mathbf{v}^s_k - \mathbf{G}^s_{k+1}\widetilde{\mathbf{w}}^s_{k+1}$ with $\mathcal{L}_k = \mathbf{I} - \mathbf{G}^s_{k+1}\widetilde{\mathbf{H}}^s_{k+1}$. The term $\widetilde{\mathbf{E}}^s_k\mathbf{q}^s_k$ has been rendered to zero by choosing $\mathbf{G}^s_{k+1}$ such that $\mathbf{G}^s_{k+1} = \mathbf{E}^s_k(\widetilde{\mathbf{H}}^s_{k+1}\mathbf{E}^s_k)^\dagger$ with † denoting Moore-Penrose Pseudo-inverse operation, which is ensured when the output measurement sensors are not less than the rejected input disturbances and accordingly the $\mathbf{H}^s_{k+1}\mathbf{E}^s_k$ is a full column matrix. Hence, Equation (10) is not dependent on the boundary measurements ($\mathbf{q}^s_k$) anymore. $\widetilde{\mathbf{v}}^s_k$ is the process uncertainty term for the revised system with covariance $(\mathbf{Q}^s + \mathbf{G}^s_{k+1}\mathbf{T}^s_{k+1}\mathbf{R}^s\mathbf{T}^s_{k+1}{}^T\mathbf{G}^s_{k+1}{}^T)$.

4.2 Marginalized particle filter

Contrary to the previously cited references, a supplementary physical parameter (θ^T) is estimated alongside the stiffness parameters (θ^E) of the model. Here, ΔT is assumed to be homogeneous within the considered subdomain system, whereas the subdomain is small enough to satisfy this homogeneity assumption.

In order to estimate the system parameters (i.e. health index and change in temperature), $\Theta(= [\theta^E\ ;\ \theta^T])$ is estimated using a set of particles ($\boldsymbol{\Theta}$) with PF, while a set of ensembles associated with each particle is utilized to estimate the state $\mathbf{x}^s_k$. Θ estimates are used to define the current system matrices and to propagate the state estimate $\mathbf{x}^s_k$ along the EnKF equations, thereby both filters (PF and EnKF) interact with each other leading to state estimates conditional to Θ.

Particle filtering. At the k^{th} iteration, prior estimates of parameters (Θ_k) are propagated through a state evolution equation with PF using a set of N_p parameter particles, $\boldsymbol{\Theta}_k = [\Theta^1_k\ \Theta^2_k\ \cdots\ \Theta^{N_p}_k]$. Each j^{th} particle is evolved through a random perturbation around its current position. Different strategies for the evolution of the particles are discussed in Sen et al. (2021) which yields the chosen $\boldsymbol{\Theta}^j_{k+1} = \beta\boldsymbol{\Theta}^j_k + \mathcal{N}(\delta\boldsymbol{\Theta}_{k+1}, \sigma^{\boldsymbol{\Theta}}_{k+1})$. β is a hyper-parameter, tuning the turbulence in Θ estimation.

Further, propagated particles are passed through EnKF for state evolution. Eventually, the particles evolve based on their estimated likelihood depending on the current output. Thus, the particle evolution becomes independent of the initial distribution of $\boldsymbol{\Theta}$.

Ensemble Kalman filtering. For the j^{th} particle, N_e ensembles are passed through EnKF for state evolution, where the state is initialized at zero for each ensemble. Meanwhile, $\mathbf{u}^s_0$ is realized as an SWGN with $\mathbf{Q}^s_u$ being its variance for the ensemble propagation. The state prediction equation along with the transformed measurement equation for the i^{th} ensemble of the j^{th} particle is given by,

$$\begin{aligned}\mathbf{x}^{s^{i,j}}_{k+1|k} &= \widetilde{\mathbf{A}}^{s^j}_k\mathbf{x}^{s^{i,j}}_{k|k} + \widetilde{\mathbf{B}}^{s^j}_k\mathbf{u}^{s^{i,j}}_k - \mathbf{G}^{s^j}_{k+1}\widetilde{\mathbf{D}}^{s^j}_{k+1}\mathbf{u}^{s^{i,j}}_{k+1} \\ &\quad + \mathbf{G}^{s^j}_{k+1}\mathbf{z}^{s^{i,j}}_{k+1} + \widetilde{\mathbf{v}}^{s^{i,j}}_k \\ \mathbf{z}^{s^{i,j}}_{k+1|k} &= \widetilde{\mathbf{H}}^{s^j}_{k+1}\mathbf{x}^{s^{i,j}}_{k+1|k} + \widetilde{\mathbf{D}}^{s^j}_{k+1}\mathbf{u}^{s^{i,j}}_{k+1} + \widetilde{\mathbf{w}}^{s^{i,j}}_{k+1}\end{aligned} \tag{11}$$

The innovation, $\varepsilon^{i,j}_{k+1}$ corresponding to the i^{th} ensemble is calculated as the departure of the predicted measurement ($\mathbf{z}^{s^{i,j}}_{k+1|k}$) from the actual measurement (transformed). The ensemble mean of the innovations is given as, $\varepsilon^j_{k+1} = \frac{1}{N_e}\sum_{i=1}^{N_e}\varepsilon^{i,j}_{k+1}$.

The predicted state and transformed measurement error covariance, $C^{j,xz}_{k+1}$, and the transformed measurement error covariance, $\mathbf{S}^j_{k+1}$, are given by,

$$\begin{aligned}C^{j,xz}_{k+1} &= \frac{1}{N_e-1}\sum_{i=1}^{N_e}\left(\mathbf{x}^{s^j}_{k+1|k} - \mathbf{x}^{s^{i,j}}_{k+1|k}\right)\left(\mathbf{z}^{s^j}_{k+1|k} - \mathbf{z}^{s^{i,j}}_{k+1|k}\right)' \\ \mathbf{S}^j_{k+1} &= \frac{1}{N_e-1}\sum_{i=1}^{N_e}\left(\mathbf{z}^{s^j}_{k+1|k} - \mathbf{z}^{s^{i,j}}_{k+1|k}\right)\left(\mathbf{z}^{s^j}_{k+1|k} - \mathbf{z}^{s^{i,j}}_{k+1|k}\right)' \\ &\quad + \mathbf{T}^s_{k+1}\mathbf{R}^s\mathbf{T}^{s'}_{k+1}\end{aligned} \tag{12}$$

where, $\mathbf{x}^{s^j}_{k+1|k}$ and $\mathbf{z}^{s^j}_{k+1|k}$ are the ensemble mean of the predicted states and transformed measurements, respectively. Further, the EnKF gain is obtained as, $\mathbb{G}^j_{k+1} = C^{j,xz}_{k+1}(\mathbf{S}^j_{k+1})^{-1}$. The state ensembles are updated as $\mathbf{x}^{s^{i,j}}_{k+1|k+1}$,

$$\mathbf{x}^{s^{i,j}}_{k+1|k+1} = \mathbf{x}^{s^{i,j}}_{k+1|k} + \mathbb{G}^j_{k+1}\varepsilon^{i,j}_{k+1} \tag{13}$$

Further, the ensemble mean, $\mathbf{x}^{s^j}_{k+1|k+1}$, of the updated states is calculated as, $\mathbf{x}^{s^j}_{k+1|k+1} = \frac{1}{N_e}\sum_{i=1}^{N_e}\mathbf{x}^{s^{i,j}}_{k+1|k+1}$.

Particle approximation. With ε^j_{k+1} and $\mathbf{S}^j_{k+1}$, the likelihood of each particle is computed as, $\mathbb{L}(\boldsymbol{\Theta}^j_{k+1}) = \frac{1}{\sqrt{|\mathbf{S}^j_{k+1}|}}e^{-0.5\varepsilon^j_{k+1}{}^T\mathbf{S}^j_{k+1}{}^{-1}\varepsilon^j_{k+1}}$. The normalized weight for the j^{th} particle is

$$w(\boldsymbol{\Theta}^j_{k+1}) = \frac{w(\boldsymbol{\Theta}^j_k)\mathbb{L}(\boldsymbol{\Theta}^j_{k+1})}{\sum_{j=1}^{N_p}w(\boldsymbol{\Theta}^j_k)\mathbb{L}(\boldsymbol{\Theta}^j_{k+1})} \tag{14}$$

Finally, particle approximations for states and parameters are estimated as weighted means,

$$\begin{aligned}\mathbf{x}^s_{k+1|k+1} &= \sum_{j=1}^{N_p}w(\boldsymbol{\Theta}^j_{k+1})\mathbf{x}^{s^j}_{k+1|k+1} \quad \text{and} \\ \Theta_{k+1} &= \sum_{j=1}^{N_p}w(\boldsymbol{\Theta}^j_{k+1})\boldsymbol{\Theta}^j_{k+1}\end{aligned} \tag{15}$$

5. NUMERICAL VALIDATION ON A STRUCTURAL SIMPLY SUPPORTED BEAM

The proposed methodology in Section 4 has been tested on a mechanical system as an example. A numerical study has been undertaken on a prismatic simply supported beam, replicated as a 2 Dimensional (2D) Euler-Bernoulli beam finite element model (FEM). For the details on the considered steel beam, refer to Table 1. The beam is divided

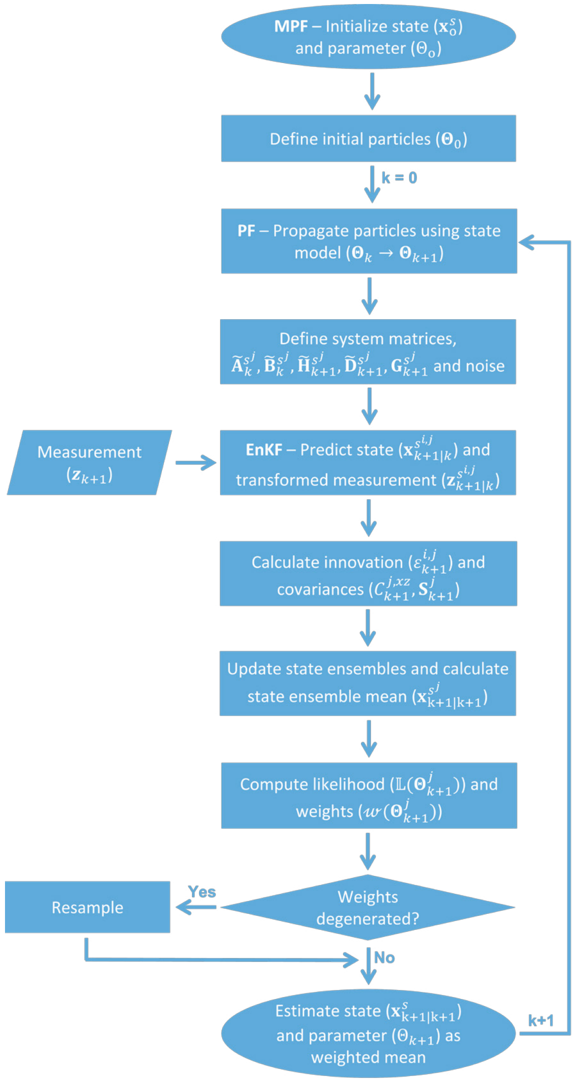

Fig. 1. Flowchart of the proposed methodology

into 10 equal parts and each part is defined by 4 *dof* FEM beam elements. Further, a subdomain/substructure [1], M_5 is considered which is divided into 6 substructural elements of equal length, cf. Figure 2.

Table 1. Properties of simply supported beam

Length of beam	$3\ m$
Cross-section area of beam	$0.013 \times 0.013\ m^2$
Elasticity of beam	$200\ GPa$
Density of beam	$7850\ Kg/m^3$
Damping ratio	0.02

Measurement data is collected on all the dofs, which are all excited by an SWGN external force ($\mathcal{N}(0, 10)\ N$). An external ambient temperature field is applied to the structure, cf Table 2.

Table 2. Temperature distribution

M_1	M_2	M_3	M_4	M_5	Substructure
30	25	30	30	40	$T(°C)$
M_6	M_7	M_8	M_9	M_{10}	Substructure
30	40	25	40	30	$T(°C)$

[1] the terms subdomain and substructure bearing the same meaning has been used interchangeably

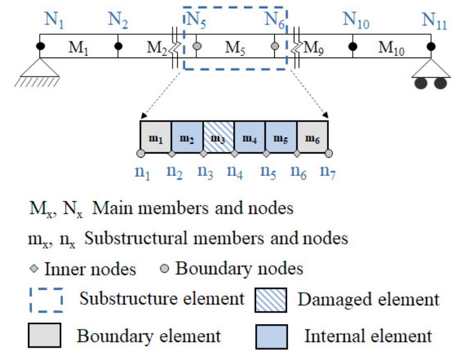

Fig. 2. 2D simply supported beam model with its substructural element, M_5

A 40% damage is induced in m_3 substructural element of substructure M_5, throughout the simulation. The measurement response is obtained for 1024 data points at a sampling frequency of 50 Hz. A 1% signal-to-noise ratio (SNR) has been added to the simulated measurement to mimic responses obtained from real-life experiments.

Response data corresponding to only the substructural nodes, $\{n_2 : n_6\}$ (cf. Figure 2) has been provided to the proposed algorithm for damage detection. For parameter estimation, 1500 particles have been selected, whereas 50 ensembles have been utilized for state estimation. The initial particle distribution type corresponding to θ^E parameters is Gaussian with a mean value of 1 and a standard deviation of 0.03. Further, the initial distribution for particles corresponding to θ^T is given by $\mathcal{N}(5, 5)$, whereas its standard deviation is changed to 0.5 after 20 iterations to control the turbulence in θ^T estimation. β has been set to 0.99 to control the weight of prior belief in parameter estimation.

In the absence of the proposed approach, if a regular MPF is utilized for parameter estimation corresponding to a subdomain system, the algorithm may malfunction. Figures 3 and 4 show that the MPF without the Kitanidis filter is incapable of a proper estimation of parameter $\boldsymbol{\Theta}$.

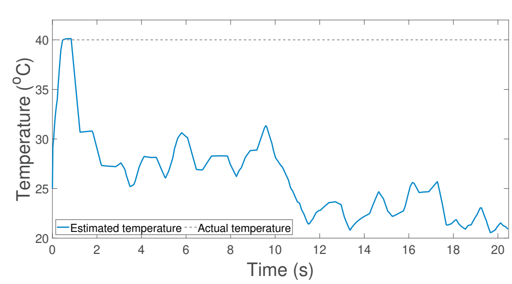

Fig. 3. Estimation of ambient temperature in substructure M_5: MPF only

Simultaneous estimation of health indices (θ^E) and ΔT (θ^T) is carried out with the help of the proposed algorithm. Figure 5 depicts the estimated ambient temperature which is given as the sum of the reference temperature ($= 20°C$) and parameter ΔT (θ^T). The ambient temperature smoothly converged to its actual value of $40°C$. Notice that damage is polled for each substructural element, T is estimated for the entire substructure under consideration and no other neighboring substructures are analyzed. No information is assumed known about the external environ-

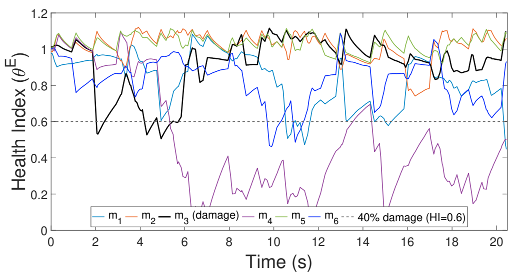

Fig. 4. Estimation of health indices of substructural elements – $m_1 : m_6 \in M_5$ with m_3 damaged: MPF only

mental conditions and their impact on the physical model outside the considered substructure. This information is not estimated nor needed due to the robustness properties of the output injection approach. Further, the estimation of θ^E has been illustrated in Figure 6, where a value of about 0.6 has been estimated for the substructural element m_3 corresponding to damage of 40% of its original value. The proposed approach has promptly and accurately estimated the damage present in the correct element without any false alarm. Finally, for both the undamaged and damaged substructural elements of M_5, Figure 7 shows the particle evolution, in terms of the variation of their corresponding mean and standard deviation. Following this, $\theta^E < 0.8$ can be set as a threshold for the presence of fault identification.

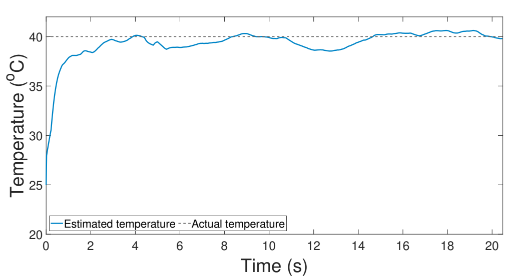

Fig. 5. Estimation of ambient temperature in substructure M_5: The proposed approach

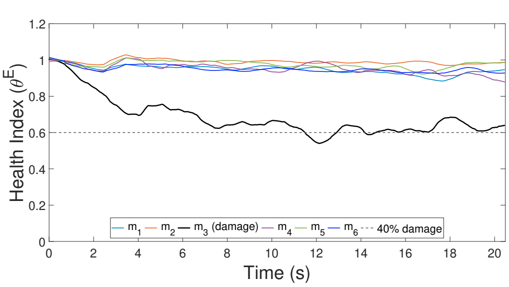

Fig. 6. Estimation of health indices of substructural elements – $m_1 : m_6 \in M_5$: proposed approach

6. CONCLUSION

In this paper, a coupled marginalized filter and a simplified sub-optimal version of Kitanidis output injection filter for robustness to unknown boundary conditions have been presented. The algorithm is able to localize and quantify a fault in a given subsystem of the monitored system while being robust to changes in the local and non-local environmental conditions. The future scope of the present study may include but is not limited to the implementation

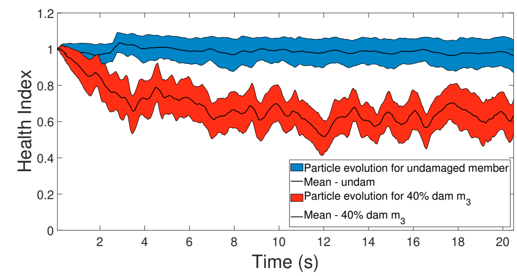

Fig. 7. Particle evolution for the damaged and undamaged substructural members: proposed approach

of the methodology on real-life complex structures such as bridges with an in-depth performance study under real-life process and measurement uncertainties.

REFERENCES

Carden, E. and Fanning, P. (2004). Vibration based condition monitoring: a review. *Structural Health Monitoring*, 3(4), 355–377.

Deraemaeker, A., Reynders, E., De Roeck, G., and Kullaa, J. (2008). Vibration-based structural health monitoring using output-only measurements under changing environment. *Mechanical Systems and Signal Processing*, 22(1), 34–56.

Kankanamge, N.D. and Mahendran, M. (2011). Mechanical properties of cold-formed steels at elevated temperatures. *Thin-Walled Structures*, 49(1), 26–44.

Karlsson, R., Schon, T., and Gustafsson, F. (2005). Complexity analysis of the marginalized particle filter. *IEEE Transactions on Signal Processing*, 53(11), 4408–4411. doi:10.1109/TSP.2005.857061.

Kitanidis, P.K. (1987). Unbiased minimum-variance linear state estimation. *Automatica*, 23(6), 775–778.

Koh, C.G., See, L.M., and Balendra, T. (1991). Estimation of structural parameters in time domain: a substructure approach. *Earthquake Engineering & Structural Dynamics*, 20(8), 787–801.

Liu, C.Y. and DeWolf, J.T. (2007). Effect of temperature on modal variability of a curved concrete bridge under ambient loads. *Journal of Structural Engineering*, 133(12), 1742–1751.

Schon, T., Gustafsson, F., and Nordlund, P. (2005). Marginalized particle filters for mixed linear/nonlinear state-space models. *IEEE Transactions on Signal Processing*, 53(7), 2279–2289.

Sen, S., Aswal, N., Zhang, Q., and Mevel, L. (2021). Structural health monitoring with non-linear sensor measurements robust to unknown non-stationary input forcing. *Mechanical Systems and Signal Processing*, 152, 107472.

Sohn, H. (2007). Effects of environmental and operational variability on structural health monitoring. *Philosophical Transactions of the Royal Society A: Mathematical, Physical and Engineering Sciences*, 365(1851), 539–560.

Zghal, M., Mevel, L., and Del Moral, P. (2014). Modal parameter estimation using interacting kalman filter. *Mechanical Systems and Signal Processing*, 47(1-2), 139–150.

Zhang, Q. and Zhang, L. (2018). State estimation for stochastic time varying systems with disturbance rejection. *IFAC-PapersOnLine*, 51(15), 55–59.